Tuberization in Potato Involves a Switch from Apoplastic to Symplastic Phloem Unloading

Roberto Viola,[a,1] Alison G. Roberts,[b] Sophie Haupt,[b] Silvia Gazzani,[a,c] Robert D. Hancock,[a] Nelson Marmiroli,[c] Gordon C. Machray,[d] and Karl J. Oparka[b]

[a] Unit of Plant Biochemistry, Scottish Crop Research Institute, Invergowrie, Dundee DD2 5DA, United Kingdom
[b] Unit of Cell Biology, Scottish Crop Research Institute, Invergowrie, Dundee DD2 5DA, United Kingdom
[c] Department of Evolutionary Biology, University of Parma, Viale delle Scienze, 43100 Parma, Italy
[d] Unit of Gene Expression, Scottish Crop Research Institute, Invergowrie, Dundee DD2 5DA, United Kingdom

Phloem unloading was studied in potato plants in real time during the early stages of tuberization using carboxyfluorescein (CF) as a phloem-mobile tracer, and the unloading pattern was compared with autoradiography of tubers that had transported ^{14}C assimilates. In stolons undergoing extension growth, apoplastic phloem unloading predominated. However, during the first visible signs of tuberization, a transition occurred from apoplastic to symplastic transport, and both CF and ^{14}C assimilates subsequently followed identical patterns of phloem unloading. It is suggested that the switch to symplastic sucrose unloading may be responsible for the upregulation of several genes involved in sucrose metabolism. A detailed analysis of sugar levels and ^{14}C sugar partitioning in tuberizing stolons revealed a distinct difference between the apical region of the tuber and the subapical region. Analysis of invertase activity in nontuberizing and tuberizing stolons revealed a marked decline in soluble invertase in the subapical region of swelling stolons, consistent with the switch from apoplastic to symplastic unloading. However, cell wall–bound invertase activity remained high in the apical 1 to 2 mm of tuberizing stolons. Histochemical analysis of potato lines transformed with the promoter of an apoplastic invertase gene (*invGE*) linked to a reporter gene also revealed discrete gene expression in the apical bud region. Evidence is presented that the apical and lateral tuber buds function as isolated domains with respect to sucrose unloading and metabolism.

INTRODUCTION

The potato tuber functions as a massive storage reserve for a range of macromolecules, most notably starch and protein. During growth of the main potato stem, underground lateral shoots (stolons) characterized by elongated internodes, hooked apical tips, and diageotropic growth (Cutter, 1978) develop. Following specific environmental cues, including short photoperiod, high light intensity and low nitrogen levels, the stolons are induced to form tubers (Ewing and Struik, 1992). The transformation of stolons into tubers impacts greatly on the physiology of the entire plant, because the developing tubers subsequently become the largest sinks present (Oparka, 1985). During the early stages of tuber formation the stolons alter their growth habit, displaying a cessation of elongation growth and the initiation of subapical radial growth (Cutter, 1978). Increased cell division and expansion is followed rapidly by a massive deposi-

tion of starch and storage proteins, such as patatin, as a result of the coordinated expression of genes involved in starch and protein biosynthesis (Prat et al., 1990; Visser et al., 1994).

Many changes have been documented to occur in stolon tips during tuber initiation. In nonswelling stolons undergoing elongation growth, cell division is observed in the apical and subapical region, up to a distance of ~5 mm from the apex (Xu et al., 1998). Upon tuber initiation, cessation of stolon growth coincides with the cessation of mitotic activity in the apical meristem (Leshem and Clowes, 1972; Xu et al., 1998; Vreugdenhil et al., 1999) and the onset of dormancy (Wiltshire and Cobb, 1996). The earliest changes associated with tuber formation are a marked increase in both radial expansion and mitotic index of cells (Vreugdenhil et al., 1999) in the subapical stolon region concomitant with the deposition of starch and protein (Ewing and Struik, 1992; Xu et al., 1998). There have been many studies of the effects of growth regulators on tuberization in potato, but no unequivocal "tuberizing" factor has been identified (Jackson, 1999). This is perhaps due to the fact that the tuberizing process consists of a complex sequence of independently regulated

events (Ewing and Struik, 1992; Jackson, 1999). For example, the arrest of stolon growth (Vreugdenhil and Struik, 1989), initiation of radial growth (Catchpole and Hillman, 1969; Mingo-Castel et al., 1976) and storage polymer deposition (Park, 1990; Müller-Röber et al., 1992) are all events that have been shown to be capable of occurring independently of each other.

Although sucrose is the main translocated sugar in potato (Oparka and Prior, 1987), there is no consensus as to whether sucrose levels increase in stolon tips at the onset of tuber formation (Davies, 1984; Hajirezaei et al., 2000). It is known that the glucose:fructose ratio increases markedly in stolon tips at tuberization (Davies, 1984), a process that has been attributed to the induction of fructokinase (Davies and Oparka, 1985; Ross et al., 1994). This enzyme is often linked with the operation of the sucrose synthase (SuSy)–mediated pathway (Davies and Viola, 1994), because fructose is an inhibitor of SuSy activity (Gardner et al., 1992). SuSy activity markedly increases during tuberization whereas acid invertase levels decrease (Appeldoorn et al., 1997), suggesting that a switch occurs in the sucrolytic pathway as elongating stolons begin to form tubers.

Despite numerous studies of carbohydrate partitioning in the potato plant, the pathway of phloem unloading in the tuber remains equivocal. In a study of tuberizing stolons, Oparka (1986) found that plasmodesmata connected the sieve element–companion cell (SE-CC) complexes of the phloem with the surrounding storage parenchyma elements, providing a structural basis for symplastic phloem unloading. Subsequent work on growing tubers in situ revealed that plasmolysis of tuber tissues had an inhibitory effect on the unloading of ^{14}C-sucrose from the phloem, supporting a symplastic phloem-unloading pathway (Oparka and Prior, 1987). However, isolated discs from potato tubers show a considerable capacity for the uptake of sucrose from the surrounding medium (Oparka and Wright, 1988, Oparka et al., 1992). Transgenic expression of yeast acid invertase in the apoplast of growing tubers significantly affected tuber yield (Sonnewald et al., 1997), further indicating that apoplastic sucrose levels may be important after phloem unloading. Oparka et al. (1992) interpreted the presence of sucrose in the apoplast as a result of leakage from recipient sink cells rather than an obligatory step in the SE-unloading process and suggested that symplastic sucrose unloading may involve subsequent leakage to the apoplast with a concomitant retrieval of sucrose into storage cells via membrane carriers. However, the importance of apoplastic sucrose retrieval on tuber yield appears to be marginal, as shown by tuber-specific antisense repression of the sucrose transporter (*SUT1*; unpublished results cited in Frommer and Sonnewald, 1995).

To date, research has focused on the transport and metabolism of sucrose in growing tubers. The mechanisms of solute translocation in stolon tips before or during tuber initiation are much less understood. Transgenic approaches have not helped in this respect because the class 1 patatin B33 promoter, used often to design tuber-specific constructs, appears to be inactive in stolons and during the early stages of tuber formation (Tauberger et al. 1999). Because the mechanism of phloem unloading during early tuber growth remains unresolved, we have investigated in detail the pathway of sucrose unloading in stolon tips before and during early tuber formation. Using a combination of confocal microscopy, autoradiography, and biochemical analyses, we provide evidence that apoplastic sucrose unloading predominates during the elongation phase of stolon growth. However, during the first observable phases of tuberization, a transition occurs from apoplastic to symplastic phloem unloading that is accompanied by a marked decline in soluble acid invertase activity. Throughout the remainder of tuber growth, symplastic phloem unloading predominates. We also provide evidence that cell wall–bound invertase activity and the expression from a promoter of an apoplastic invertase gene is maintained in the dormant apical bud of developing tubers, suggesting that this region functions as a discrete cellular domain with regard to sucrose unloading and metabolism.

RESULTS

Developing Stolons

Plants removed from soil before the onset of tuberization showed typical stolon morphology, including a hooked apical tip. In these stolons, longitudinal growth was still occurring, and no sign of swelling was evident at the stolon tip (Figure 1A). For experimental purposes, these stolons were split into three areas, namely, the apical region (tip), the "hook," and the subapical region (Figure 1A). For tissue sampling purposes, the stolons were cut transversely into 1-mm-thick sections from the tip through the subapical region (Figure 1A).

Potato plants harvested between 8 and 10 weeks after planting produced both nonswelling and swelling stolon tips. Depending on their developmental stage, some plants had only nonswelling stolons, whereas others produced a range of both swelling and nonswelling stolon tips (Figure 1B).

Unloading of Carboxyfluorescein and ^{14}C Assimilates

Carboxyfluorescein (CF) was used as a fluorescent marker of phloem transport and symplastic phloem unloading (Roberts et al., 1997), and its behavior was compared with the pattern of assimilate unloading, as determined by autoradiography. Figures 2 and 3 show stolons or developing tubers of different growth stages that had imported either CF or ^{14}C. Figures 2A and 2B show a longitudinal section through elongating stolons. In such nonswelling stolons, CF was found

Figure 1. Stolon Tips of Potato (cv Desire) Showing Regions Taken for Analysis of Phloem Unloading and Sucrose Metabolism.

(A) Note the prominent stolon hook, which marks a clear distinction between apical and subapical regions. Segments taken for analyses are indicated on the stolon.

(B) Tuberizing stolon tips taken from a single plant. A number of distinct stages in the swelling process are apparent, ranging from no swelling (1) to prominent subapical swelling (4). Note the progressive incorporation of the apical bud into the growing tuber.

Bars in **(A)** and **(B)** = 1 mm.

only in the phloem of vascular bundles and was not unloaded into surrounding parenchyma cells, either along the phloem pathway or in the apical region of the stolon (Figure 2A). In contrast, in autoradiographs, relatively uniform labeling was apparent across the entire stolon diameter (Figure 2B), indicating that, unlike CF, radiolabeled assimilates had been unloaded from the phloem and distributed throughout stolon tissues. In stolons that had begun to swell (stage 2 in Figure 1B), CF was restricted to the phloem within the stolon axis and also within the swelling portion of the stolon (Figure 2C), a feature reflected in the distribution of ^{14}C (Figure 2D). At this early stage of tuberization, little CF or ^{14}C was detected in the apical region of the stolon hook (cf. Figure 2C with Figure 2D). Later in development, as the swellings became larger (corresponding to stage 3 in Figure 1B), subdivision of the phloem into numerous internal strands was apparent (Figures 2E and 2F). These strands ramified throughout the perimedulla and cortex of the developing tuber, creating a complex phloem network among the storage tissues (Artschwager, 1924). In the developing tubers shown in Figures 2E and 2F, a clear distinction is apparent between the transport phloem of the stolon and the unloading phloem of the developing tuber. With continued tuber enlargement (stage 4 and larger, Figure 1B), the subdividing phloem within the tuber was more clearly apparent (Figures 2G to 2J), and unloading of CF occurred from both internal and external phloem systems (Figure 2I). In transverse sections of developing tubers, symplastic phloem unloading of CF was clearly apparent (Figure 2K), a pattern that mirrored the unloading of ^{14}C (Figure 2L).

In transverse sections, distinct differences were observed in the distribution of CF in nontuberizing and tuberizing sto-

lons (Figures 3A and 3B). In the stolon, CF was clearly restricted to transport phloem on either side of the xylem cylinder. In small tubers, which had recently commenced swelling, the internal and external phloem strands had begun to proliferate and separate, and CF was seen to spread in a diffuse pattern away from the phloem strands (Figure 3B). In the tuber shown in Figure 3C, the xylem of the detached tuber was labeled by immersing the cut end of the stolon in a solution of Texas Red dextran. Note that the xylem formed a discrete ring separating the internal and external phloem strands, with little dye leakage to the apoplast. As the tubers continued to swell, the inner and outer phloem strands became separated by the formation of intervening parenchyma tissues (Figure 2C; see also Artschwager, 1924). A similar pattern of ^{14}C distribution was seen after autoradiography (Figure 2L). In some instances, the internal phloem was more heavily labeled than the outer phloem, or vice versa (cf. Figures 2K and 2L). These differences most likely reflect the extent to which internal and external phloem systems of the leaf became labeled with CF and ^{14}C assimilates, respectively. Differences in CF unloading were apparent along the length of a single tuber. Figure 3D shows transverse sections taken sequentially from stolon (left) to tuber tip (right) of the same swelling tuber. Note that dye unloading is most prolific in the subapical region of the tuber.

Aborted Tubers Do Not Unload CF

A characteristic feature within a population of tuberizing stolons is a small fraction of stolons that initiate tubers that subsequently fail to grow, possibly due to intense competition for assimilates (Oparka, 1985). Such tubers were identified here and were usually initiated close to the soil surface. An interesting feature in many of these tubers was their inability to unload either CF or ^{14}C from the phloem (Figures 3E and 3F). These results suggest that the abortion of such tubers does not impair the ability of the phloem to import CF or assimilates but rather to unload them. The above observation also demonstrates that CF does not leak from the phloem when the symplastic unloading mechanism is impaired.

Dormant Apical Buds Are Symplastically Isolated

Irrespective of the developmental stage of swelling tubers, CF was not found at the apex of the tuber within the dormant apical bud, a feature mirrored in autoradiographs (e.g., Figure 2F). The resolution of the ^{14}C autoradiographs could not be improved, but a closer examination of the apical buds in growing tubers unloading CF showed that phloem connections were present immediately below, and leading into, the apical bud (Figure 3G). However, unloading did not occur from the phloem in this region, giving the phloem a more clearly defined outline than that found in surrounding
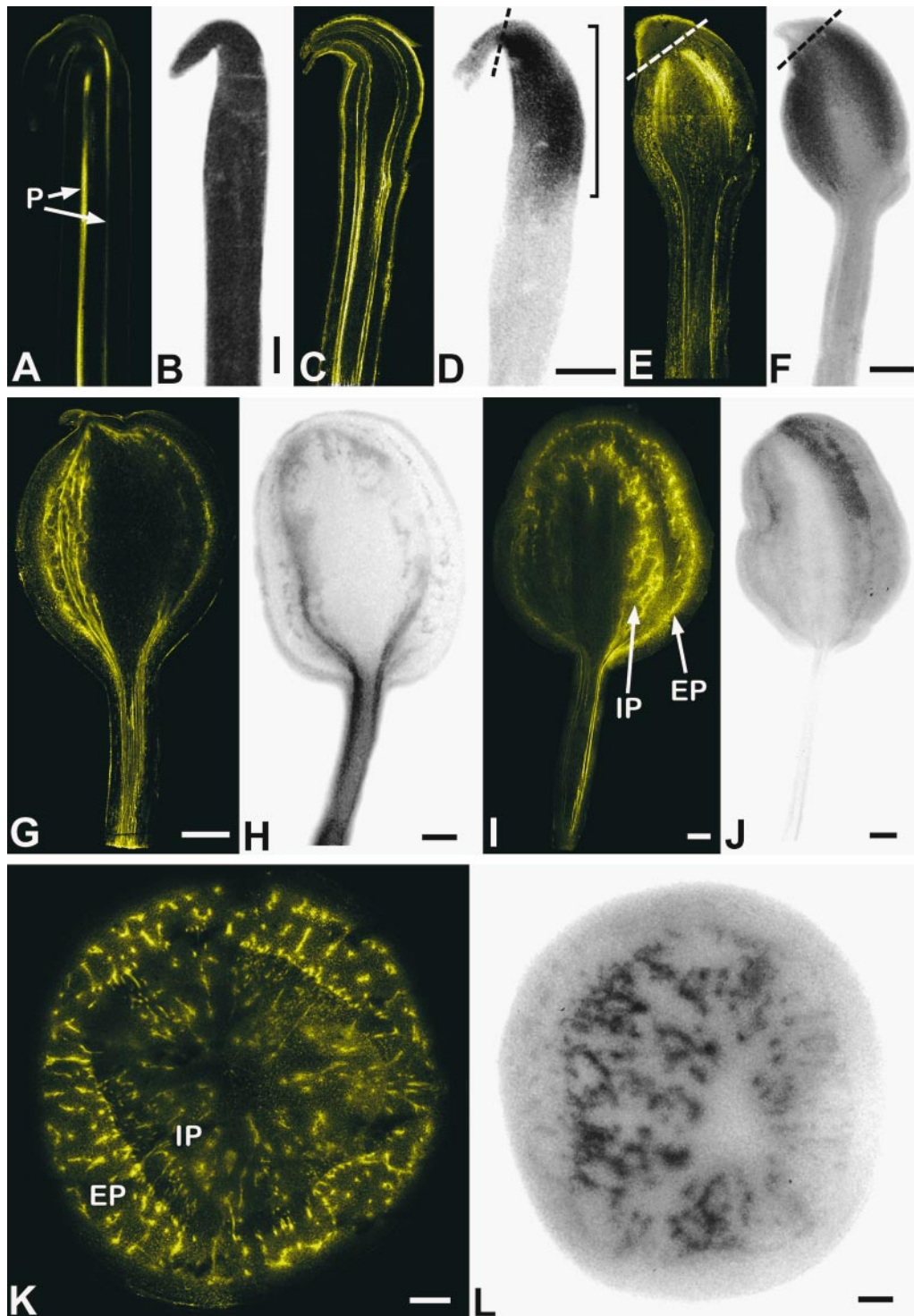
Figure 2. Confocal Laser Scanning Microscopy of CF Unloading in Comparison with [14]C Autoradiography.

(A) In nonswelling stolons, CF was restricted to the phloem (P) in both the stolon axis and hook regions.
(B) In stolons of the same developmental stage, ^{14}C was distributed evenly across the stolon axis and hook.
(C) In stolons showing the first detectable subapical swelling, CF remained confined to the phloem strands.

storage tissues. Similar observations were made on dormant lateral buds arising some distance behind the apex (Figure 3H).

Unloading of Labeled Assimilates and Metabolism of ^{14}C-Sucrose

Tuberizing and nontuberizing potato plants were exposed to $^{14}CO_2$ for 1 hr, and the concentration of labeled assimilates in the apical 15 mm of stolon axes was determined 24 hr later. The profile of label distribution along the longitudinal axis of stolons at different developmental stages is shown in Figure 4. To show the principal changes that occurred during tuberization, the tuberizing stolons have been grouped into "small" swelling stolons (2 to 5 mm diameter) and "large" swelling stolons (6 to 10 mm diameter). The concentration of radioactivity was significantly higher in swelling stolons compared with nonswelling stolons, particularly in the subapical area. The most apical (1 to 2 mm) region of swelling stolons, which incorporated the dormant apical bud, showed relatively low levels of radioactivity compared with the subapical (2 to 8 mm) region, reflecting the distribution of ^{14}C observed by autoradiography (see Figures 2D and 2F).

Sugar Content along the Stolon Axis

Figure 5 shows the sucrose, glucose, and fructose content along the longitudinal axis of nonswelling stolons, small swelling stolons, and large swelling stolons. Sucrose was the most abundant sugar in the most apical section of nonswelling stolons, and its concentration gradually declined along the axis (Figure 5A). In the case of small swelling stolons, the sucrose concentration was significantly higher throughout the apical 14 mm of the stolon, particularly within the 5 mm closest to the tip. In large swelling stolons, a similar phenomenon was seen, but with a more pronounced increase in sucrose concentration throughout the swelling region. Comparing the sucrose levels shown in Figure 5 with the concentrations of incorporated radioactivity shown in Figure 4 reveals a correlation between sucrose and ^{14}C incorporation. Concentrations of glucose showed a similar pattern in all developmental stages, namely, very low levels in the most apical region (1 to 2 mm) followed by a marked rise in concentration within subapical (swelling) regions (Figure 5B). Fructose levels showed a pattern similar to that of glucose in nonswelling stolons and small swelling stolons (Figure 5C), whereas in large swelling stolons, the fructose levels appeared markedly decreased, particularly in the swelling region.

Allocation of Radioactivity between Sugars in Stolons of Plants Supplied with $^{14}CO_2$

Figure 6 shows the relative radioactivity distribution within the soluble sugars pool along the axis of nonswelling stolons (Figure 6A) or large swelling stolons (Figure 6B) taken from plants treated with $^{14}CO_2$. For comparative analyses, the relative sugar profiles along the axis of nonswelling or large swelling stolons are also shown in Figures 6C and 6D, respectively. In nonswelling stolons, radioactivity was higher in monosaccharides compared with that in sucrose in all sections, with the exception of the apical 2 mm. The labeling of both glucose and fructose showed an inverse relationship to that of sucrose in the upper 10 mm of the stolon. In this region, there was a very close correlation between the relative distribution of radioactivity in individual sugars and the sugar profile along the axis (cf. Figures 6A and 6C). This indicates rapid metabolism of imported ^{14}C-sucrose and equilibration of label with the tissue sugars in this region. In the basal region of the stolon (sections 11 to 15), the proportion of radioactivity recovered in sucrose increased, and there was little correlation between radioactivity distribution in sugars and tissue sugar content. This may be explained by a high proportion of radioactivity in this region constituted by unloading of ^{14}C-sucrose from the phloem.

Figure 2. (continued).

(D) At the same stage, ^{14}C was unloaded uniformly across the subapical (bracketed) region of the tuberizing stolon. Note the decrease in labeling intensity of the apical region (acropetal to dotted line).

(E) In visibly swollen stolons, CF showed distinct subapical unloading into parenchyma tissues. Note lack of dye movement into apical tissues (acropetal to dotted line).

(F) Autoradiography of swelling stolon shows similar pattern to **(E)**. The apical region (acropetal to dotted line) again shows less labeling than subapical tissues.

(G) to **(J)** Visibly swollen tubers unloading CF and ^{14}C, respectively. Unloading is apparent from both internal (IP) and external (EP) phloem networks.

(K) Transverse section of growing tuber unloading CF. Extensive dye unloading is apparent from internal and external phloem networks.

(L) Autoradiograph of tuber at a stage of development similar to that shown in **(K)**.

Bar in **(B)** = 1 mm for **(A)** and **(B)**. Bar in **(D)** = 2 mm for **(C)** and **(D)**. Bar in **(F)** = 2 mm for **(E)** and **(F)**. Bars in **(G)** to **(J)** and **(L)** = 2 mm.
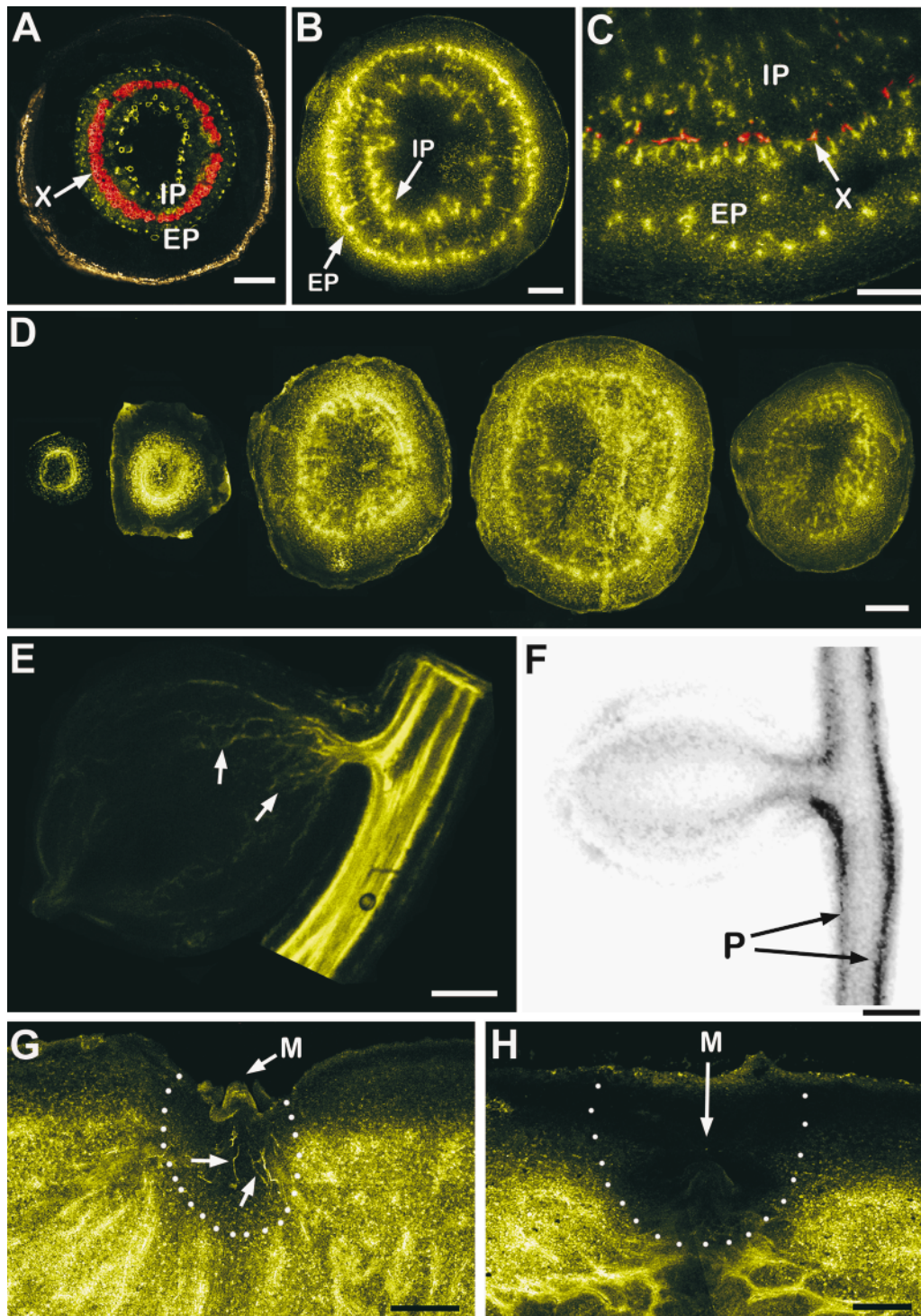
Figure 3. CF Transport and Unloading in Stolons, Aborted Tubers, and Dormant Buds.

(A) Transverse section of translocating stolon. CF is restricted to internal (IP) and external (EP) phloem systems. The functional xylem (X) was labeled with Texas Red dextran.
(B) Tuberizing stolon showing separation of internal and external phloem strands by radial expansion. Note the unloading of dye from both networks.

In large swelling stolons (Figure 6B), sucrose was the dominant form of labeled sugar in both the swelling region and the subtending stolon. In contrast to the nonswelling stolons, an inverse relationship between the levels of sucrose and monosaccharides was not apparent. In these stolons, there were also similarities in the distribution of ^{14}C between sugars along the axis and the distribution profile of soluble sugars (cf. Figures 6B and 6D), particularly with regard to sucrose and fructose. The lower incorporation into fructose in swelling stolons compared with nonswelling stolons reflected the general decline in fructose during tuber formation (see Figure 5).

Distribution of Soluble and Cell Wall–Bound Acid Invertase Activity

Figure 7 shows the activity profile of cell wall–bound (Figure 7A) and soluble (Figure 7B) acid invertase activity along the longitudinal axis of nonswelling stolons, small swelling stolons, and large swelling stolons. The profile of cell wall–bound acid invertase activity was similar in all developmental stages, showing the highest activity in the apical 2 mm. This was followed by a sharp reduction to a steady, low level of activity in the distal 8 mm. In contrast, the activity of soluble invertase in nonswelling stolons was lowest in the apical 2 mm (Figure 7B). In tuberizing stolons, a marked decline in soluble acid invertase activity was observed, except in the apical region. In large swelling stolons, the activity profiles of soluble and cell wall–bound acid invertase along the axis were similar, with the highest levels measured close to the tip.

Expression from the Promoter of an Apoplastic Invertase Gene in Stolons and Tubers[w]

Figure 8 shows expression in stolons and tubers from the promoter of an apoplastic invertase gene (*invGE*) (Maddison
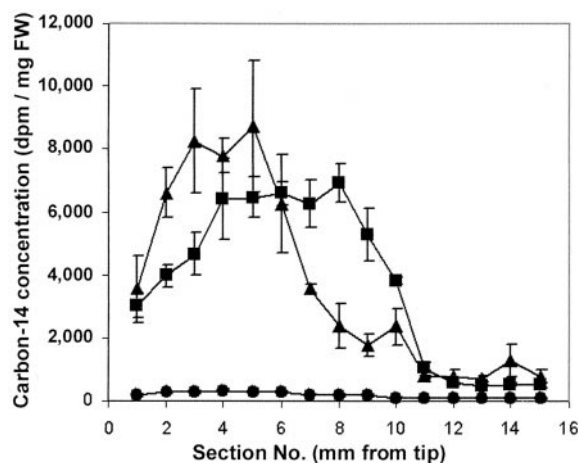

Figure 4. Concentration of Radioactivity in 1-mm Sections Excised along the Axis of Plant Stolons.

Stolons from nontuberizing plants (filled circles), small swelling stolons (2 to 5 mm diameter; filled triangles), or large swelling stolons (6 to 10 mm diameter; filled squares) are shown 4 hr after labeling of foliage with $^{14}CO_2$. Values are given as average values $\pm$ SD of stolon populations of between eight and 10 individually labeled plants. All data points for small and large swelling stolons were significantly different ($P > 0.01$) from equivalent nonswelling stolon sections. FW, fresh weight.

et al., 1999). After β-glucuronidase (GUS) staining of stolons, *invGE* promoter expression was localized strongly to the hook of developing stolons (Figure 8A). In developing tubers, *invGE* promoter expression was localized in a region of the bud subtending the apical meristem (Figure 8B). Bearing in mind the anatomical changes occurring at the apex of the stolon tips during tuberization, with the swelling subapical tissues progressively engulfing the apical region (Cutter, 1978), the localization of *invGE* expression during

---

Figure 3. (continued).

(C) Phloem unloading of CF from a sector of a large tuber. A diffuse gradient of CF is apparent from the phloem "poles." The xylem ring was labeled with Texas Red dextran.

(D) Sequential transverse sections from the same growing tuber. The stolon region is shown to the left and the tuber apex at the extreme right. Most of the CF unloading occurs from the subapical region of the tuber.

(E) An aborted tuber shows import of CF (arrows) but no unloading into surrounding parenchyma tissues.

(F) As shown in **(E)** with reduced labeling of the tuber relative to the phloem (P) of the stolon axis.

(G) The dormant apical meristem (M) shows little or no CF import. In the region subtending the meristem (encircled), dye is apparent in the phloem but appears not to have unloaded (arrows). In comparison, dye unloading is extensive into parenchyma tissues outside this region.

(H) A dormant lateral bud shows isolation similar to that described in **(G)**.

Bar in **(A)** = 0.5 mm; bars in **(B)** and **(D)** = 2 mm; bars in **(C)** and **(E)** to **(H)** = 1 mm.
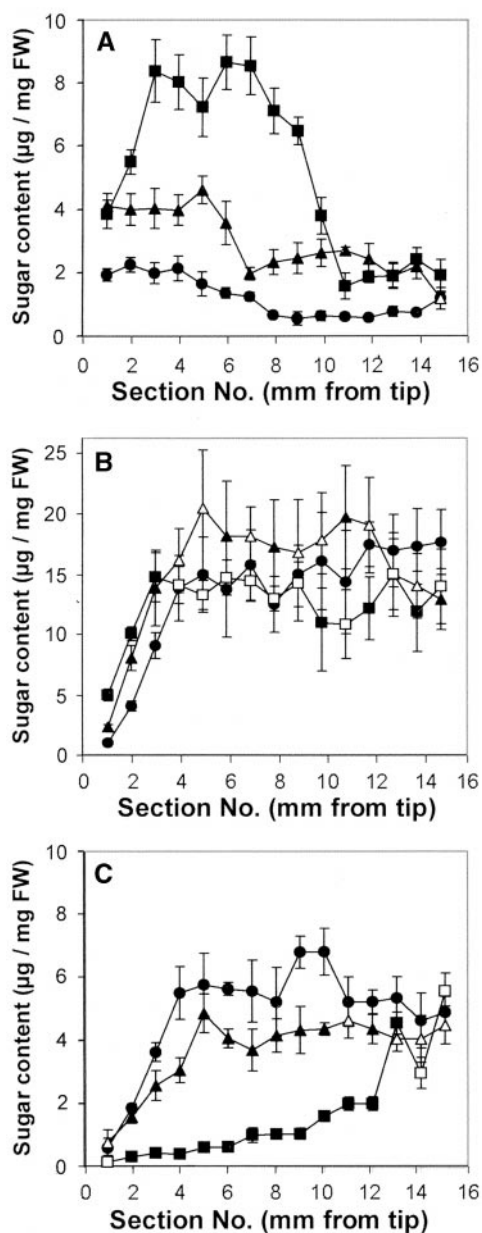
Figure 5. Soluble Sugar Content in 1-mm Sections Excised along the Axis of Nonswelling Stolons, Small Swelling Stolons, or Large Swelling Stolons.

(A) Sucrose.
(B) Glucose.
(C) Fructose.
The symbols indicate nonswelling stolons (circles), small swelling stolons (triangles) and large swelling stolons (squares). The data points represent the average values ±SD of stolon populations sampled from six nontuberizing plants (nonswelling stolons) or five tuberizing plants (swelling stolons). Data points for small or large swelling stolons that were significantly different (P > 0.01) from equivalent sections of nonswelling stolons are shown as closed symbols, and those that were not significantly different are shown as open symbols. FW, fresh weight.

tuberization appeared unchanged. This is in broad agreement with the activity profile of cell wall–bound invertase (see Figure 7A) and provides further evidence that the dormant apical region of the stolon functions as a discrete domain during tuberization.

DISCUSSION

Tuberization Involves a Switch in the Pathway of Assimilate Unloading

Confocal imaging of CF distribution in stolon tips of potato plants was used to study changes in the pathway of assimilate unloading during tuberization. A comparison of these images with ^{14}C autoradiographs provided a clear correlative picture of the phloem-unloading process during tuberization. In stolon tips there was very little or no transfer of CF to the cells surrounding the phloem, even 24 hr after CF infiltration into the foliage. In contrast, in the case of similar plants labeled with $^{14}CO_2$, there was clear evidence of unloading and metabolism of assimilates in stolon tips over the same time scale. The distribution of radioactivity in the tissue showed a strong correlation with tissue sugar composition, indicating a rapid equilibration of unloaded ^{14}C-sucrose. Based on the distribution of CF seen in the stolon tip, we conclude that sucrose synthesized in the leaves and transported to the stolons via the phloem (unlike the membrane-impermeant probe CF) is unloaded into the apoplast.

The distribution of CF in the swelling region of tuberizing stolon tips was markedly different, with substantial dye transfer occurring from the phloem to the surrounding parenchyma elements. In large tubers, the spread of CF from both the internal and external phloem into the storage tissues was conspicuous. Furthermore, in these small tubers there was a close correlation between the CF-unloading images and those obtained by autoradiography. These findings indicate that the process of tuberization is associated closely with the induction of a functional symplastic continuum between the SE-CC complexes and the parenchyma cells that form the bulk of the storage tissues. Our current observations are in agreement with previous suggestions that phloem unloading in the potato tuber is symplastic (Oparka, 1985) and adds the potato tuber to a growing list of sink organs that utilize symplastic unloading mechanisms (Fisher and Oparka, 1996; Patrick, 1997). Recent evidence from tobacco (Imlau et al., 1999; Oparka et al., 1999), Arabidopsis (Imlau et al., 1999), and wheat (Fisher and Cash-Clark, 2000) indicate that macromolecules may also be unloaded from sink tissues in these species. In the future, it will be interesting to determine the size exclusion limit for symplastic unloading in the potato tuber.
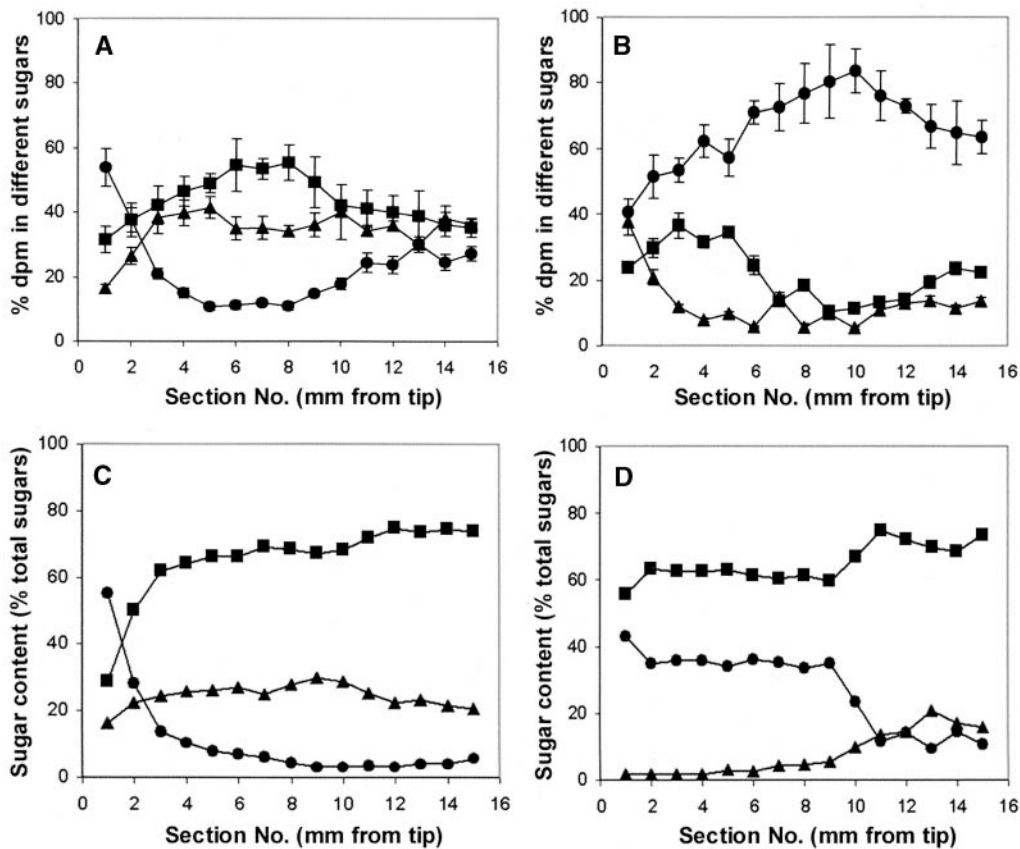
Figure 6. Relative Distribution of Radioactivity within the Soluble Sugars Pool along the Axis of Nonswelling Stolons or Large Swelling Stolons Taken from Nontuberizing and Tuberizing Plants, Respectively, 4 h after Labeling of the Foliage with $^{14}CO_2$.

(A) and **(C)** Nonswelling stolons.
(B) and **(D)** Large swelling stolons.
The symbols used indicate sucrose (circles), glucose (squares) and fructose (triangles). The data are presented as radioactivity recovered in each sugar as a percentage of the total radioactivity recovered in the soluble sugars pool (sucrose + fructose + glucose). For comparative analyses, the relative sugar distributions in each section for nonswelling stolons and swelling stolons are shown in **(C)** and **(D)**, respectively (data recalculated from Figure 4). Data for **(A)** and **(B)** are average values ±SD of eight to 10 stolons from two nontuberizing and three tuberizing plants.

Implications for Gene Regulation

It has long been known that photosynthetic rates and translocation of assimilates increase at tuber initiation (Dwelle et al., 1981; Ewing, 1990). In these experiments, we observed a significant increase in the average ^{14}C specific activity in the apical 10 mm of tuberizing stolons compared with nontuberizing stolons (4621 dpm/mg FW and 498 dpm/mg fresh weight, respectively). The increased sink potential in swelling stolon tips may be directly attributable to the switch from apoplastic to symplastic assimilate unloading in the subapical region, resulting in increased translocation rates into the tissue. The resulting increase in sucrose concentra-

tion, specifically in the symplast, is expected to impact strongly on metabolic and developmental processes. High sucrose concentrations are known to induce the transcription of several genes involved in tuber storage metabolism (Müller-Röber et al., 1990; Prat et al., 1990; Visser et al., 1994). Sucrose is also known to induce SuSy transcript levels in potato (Salanoubat and Belliard, 1989). Furthermore, SuSy activity in developing tubers shows a positive correlation with the sucrose status in the tuber (Ross and Davies, 1992). In the present work, the increased sucrose content of the swelling region of tuberizing stolon tips was correlated with a sharp decline in soluble acid invertase activity and in the rate of sucrose hydrolysis in vivo (Figures 6 and 7). Our
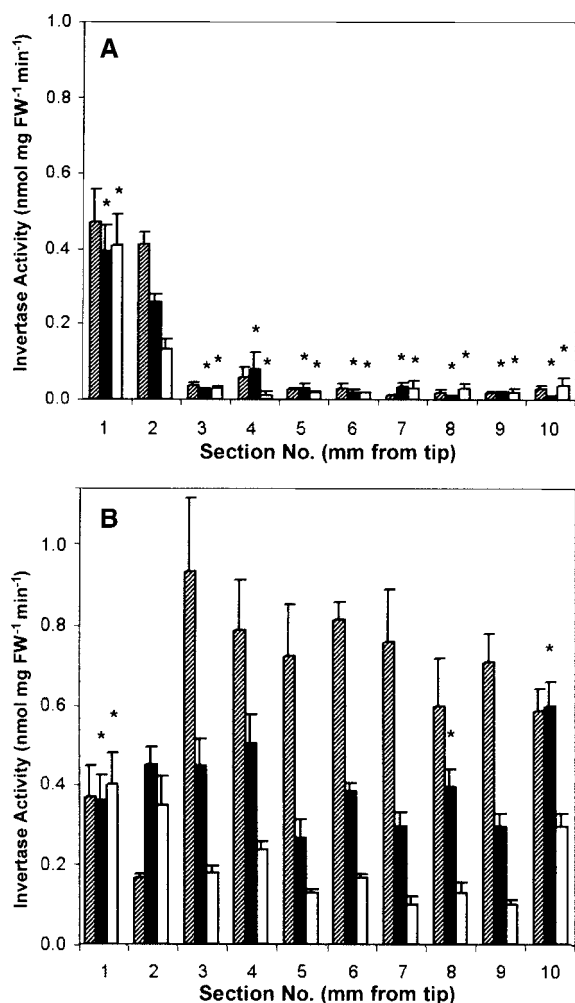
Figure 7. Distribution of Cell Wall–Bound and Soluble Acid Invertase Activity.

(A) Cell-wall bound invertase activity.
(B) Soluble invertase activity.
Activity was determined along the axis of nonswelling stolons (striped grey bars), small swelling stolons (black bars), and large swelling stolons (white bars). Data are shown as average values $\pm$SD ($n = 4$). Asterisks indicate data points that were not significantly (P > 0.01) different to equivalent sections of nonswelling stolons. FW, fresh weight.

results support the hypothesis of a switch from an invertase-sucrolytic pathway to a SuSy-sucrolytic pathway in tuberizing stolons (Ross et al., 1994; Appeldoorn et al., 1997). The induction of symplastic assimilate unloading and the decline in soluble invertase activity in the subapical region of tuberizing stolons appear to be part of a coordinated developmental program. Bearing in mind that carbohydrate status affects the regulation of invertase gene expression in

many plants (Xu et al., 1996; Sturm, 1999), it would be important to assess the effect of sugar content or composition on soluble invertase gene expression in potato stolons.

Evidence for Discrete Physiological Domains along the Stolon Axis

The induction of symplastic phloem unloading in tuberizing stolons appeared to be spatially regulated. CF was not observed in the stolon region subtending the tuber or in the nonswelling apical bud region. Autoradiographs of tuberizing stolons from plants treated with $^{14}CO_2$ also showed absence of radioactivity in the region of the apical bud. These changes may be associated with the progressive reduction in the rate of cell division in the apical meristem of the stolon, that is, with the onset of dormancy in the apical bud. This raises the possibility that the dormant apical bud may be symplastically isolated from the rest of the tuber and perhaps only becomes functionally connected to the tuber symplast at the onset of sprouting. The possibility that discrete, functional symplastic domains occur along the tuber axis was reinforced by the analysis of sugar distribution and acid invertase activity along the axis of nontuberizing and tuberizing stolons. In keeping with the observed isolation of the apical bud domain, there were sharp differences in the sugar levels of this domain when compared with subtending storage tissues. Furthermore, cell wall acid invertase was strictly localized in the apical bud region of the stolon, whereas soluble acid invertase was more abundant in the subapical region. Tuberization of stolon tips was characterized by a substantial increase in sucrose content and a marked decline of soluble invertase in the subapical (swelling) region. In contrast, there was little change in both soluble and cell wall–bound invertase activity in the most apical section (which lacked swelling) of tuberizing tips.

We propose that sucrose is unloaded from the terminal SE-CC complexes into the apoplast of developing stolon tips. In the subapical region, sucrose is retrieved by parenchyma cells via sucrose transporters, but this step is bypassed during tuber formation as a result of the establishment of symplasmic communication between the SE-CC complexes and the parenchyma cells. However, it appears that symplastic isolation may be maintained in the apical bud domain. Here, sucrose hydrolysis may occur in the free space before retrieval of hexoses, as suggested by the localization of cell wall invertase activity. This hypothesis is also supported by the highly localized expression from the *invGE* promoter in the apical region of stolons and tubers. *InvGE* is part of a family of at least four apoplastic invertase genes that have been cloned from potato (Hedley et al., 1993, 1994; Maddison et al., 1999). The expression of these genes appears highly localized; for example, *invGF* is expressed only in anthers, whereas expression of *invGE* is localized in floral tissues, in lateral nodes in the
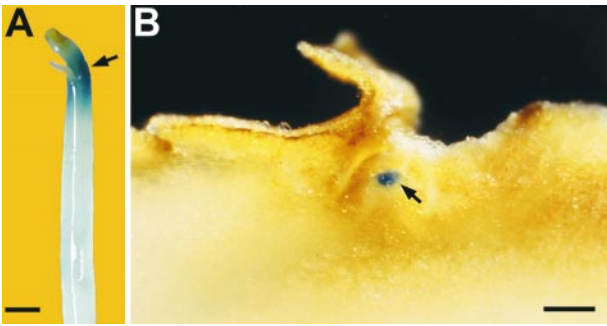
Figure 8. Expression of an Apoplastic Invertase (*invGE*) Revealed by GUS Staining.

(A) GUS staining is restricted to the apical hook region of an elongating stolon (arrow).
(B) Developing tuber showing GUS staining associated with the apical bud region (arrow).
Bar in **(A)** = 1 mm; bar in **(B)** = 500 μm.

stem (Maddison et al., 1999), and, as shown here, at the tip of elongating stolons and within dormant tuber buds. Cutter (1978) observed that a striking feature of the hooked part of the stolon tip is the highly meristematic nature of the region distal to the hook. Cell wall invertase has long been assumed to be associated with rapidly growing vegetative sinks such as meristems, where it may be involved in the hormone-mediated modulation of cell division (Ehness and Roitsch, 1997; Herbers and Sonnewald, 1998). Expression patterns of cell wall invertases in sink organs have also indicated an important role of these enzymes in sucrose metabolism during the prestorage phase (Sturm, 1999 and references therein). However, it is difficult to assign a function to apoplastic invertases during tuberization, because the expression from the *invGE* promoter and total enzyme activity remain largely unaffected during this process. The relatively low hexose content in the cell wall invertase domain also argues against a possible role for the enzyme in the maintenance of high hexose status in the apoplast of this meristematic region to stimulate mitotic activity, as shown in other systems (Weber et al., 1996; Ehness and Roitsch, 1997). Excised sections of the apical bud domain of nonswelling stolons or developing tubers show substantially faster rates of ^{14}C-hexose uptake and metabolism compared with sections of the subapical region (J. Pelloux and R. Viola, unpublished observations). Thus, the relatively higher sucrose/hexose ratio in the apical region may be attributed to a more rapid utilization of the hexoses retrieved from the free space.

Conclusions

Tuber formation is characterized by a switch from apoplastic to symplastic unloading of assimilates in the subapical region of the developing stolon. This transition in solute transport pathways results in enhanced sink potential within stolon tips and a marked change in the compartmentation of unloaded sucrose. The latter may be directly responsible for the upregulation of gene expression observed during tuber formation. These results suggest that the induction of symplastic unloading during tuber formation is a key factor in the regulation of resource allocation and sink–source relationships in potato.

METHODS

Plant Material

Tubers of *Solanum tuberosum* L. cv Desiree were planted in the field in early April. Tuberization occurred ∼48 days after planting. Experiments with nontuberizing and tuberizing plants were performed 35 to 40 days and 50 to 60 days after planting, respectively.

CFDA Labeling

To image phloem transport into developing stolons and tubers, carboxyfluorescein diacetate (CFDA; Molecular Probes, Eugene, OR) was applied to mature source leaves of either nontuberizing or tuberizing plants. Endogenous esterase activity cleaves off the diacetate moiety to leave the fluorescent, phloem-transportable carboxyfluorescein (CF) molecule (Roberts et al., 1997). Each plant was labeled with 20 mL of 1 mg mL^{-1} CFDA aqueous solution (produced from a concentrated stock in acetone). The solution was injected into the air spaces of the leaves through open stomata on the abaxial leaf surface using a plastic syringe. Plants were allowed to translocate the CF for 2 to 4 hr, and sink tissues were subsequently examined for CF fluorescence using a confocal microscope (model MRC2000; Bio-Rad, Hemel Hempstead, UK; see also Roberts et al., 1997).

Texas Red Labeling

To image xylem transport into developing stolons and tubers, we allowed cut stolons to transpire a 3-kD Texas Red dextran solution (Molecular Probes) for 30 to 60 min before examination under a confocal microscope (see also Roberts et al., 1997).

$^{14}CO_2$ Labeling

Nontuberizing or tuberizing plants were labeled with $^{14}CO_2$ to follow the subsequent movement of radioactivity into stolons and developing tubers, respectively. The plants were enclosed in large plastic bags that were sealed round the base of the stems above soil level. The radiolabel was injected into a vial inside the bag. Each plant received 1.85 MBq of $^{14}CO_2$ released from ^{14}C-bicarbonate (ICN Radiochemicals, Irvine, CA) by addition of excess 3 M lactic acid. The plants were exposed to $^{14}CO_2$ for 1 hr before injecting excess 3 M KOH to neutralize the acid and to absorb any remaining CO_2. After labeling, the plants were left for 4 hr to translocate ^{14}C to sink tissues.

Autoradiography

After $^{14}CO_2$ labeling, tissue for autoradiography was selected and sectioned before rapidly freezing in liquid nitrogen between sheets of paper. The frozen material was gently compressed between aluminum plates and freeze-dried. After drying, the tissue was pressed flat and autoradiographed using Kodak BioMax MR-1 film (Sigma, Poole, UK) at –80°C for 3 to 7 days.

Extraction and Quantification of Radioactivity

After $^{14}CO_2$ labeling, developing stolons and tubers were excised from the plants, briefly washed in distilled water to remove soil, and cut transversely into 1-mm-thick sections. For estimation of total radioactivity in the tissue, each section was weighed, and the tissue was dropped immediately into 1 mL of 80% (v/v) ethanol and extracted on an orbital shaker for 20 hr. Subsequently, 4 mL of scintillation fluid (Ecoscint A; International Diagnostics, Atlanta, GA) were added, and the mixture was mixed thoroughly before scintillation counting in a Tri-Carb liquid scintillation analyzer (model 2000CA; Packard, Meriden, CT).

Extraction and Analyses of Soluble Sugars

Tissue sections were obtained as described above and immediately immersed in boiling 80% (v/v) ethanol. The tissue was exhaustively extracted until the medium was reduced to the aqueous phase. The extract was then decanted, and the procedure was repeated twice more. The extracts were combined and reduced to 1 mL under reduced pressure, and soluble sugars were quantified enzymatically using the method of Viola and Davies (1992), with the modifications described by Mitchell et al., (1998). For determination of radioactivity in individual sugars, the samples were passed through prepacked anion exchange (SAX) and cation exchange (SCX) cartridges (100-mg cartridges; HPLC Technology, Macclesfield, UK) in sequence. The cartridges were washed with 3 mL of distilled water, and the combined unbound fractions were lyophilized. The lyophilized samples were resuspended in 0.3 mL distilled water and used for HPLC separation of individual sugars, as described (Viola, 1996), except that radioactivity was detected using a flow scintillation detector (model 150 TR; Packard) equipped with a homogeneous flow cell (500 μL). Scintillant (Ultima-Flo M cocktail, Packard) was mixed with the column eluate at a rate of 3 mL min^{-1} immediately before entry to the flow cell.

Enzyme Extraction and Assay

Stolons or tubers were sectioned as described above, and the sections were extracted in 3 volumes of ice-cold 100 mM sodium acetate, pH 5.0, containing 10 mM sodium sulphite and 2 mM phenylmethylsulfonyl fluoride. After centrifugation at 20,000g for 20 min at 4°C, the supernatant was removed, and the pellet was reextracted twice in the original volume of extraction buffer. The combined extracts were desalted using Sephadex G25 columns (Pharmacia, Uppsala, Sweden) and assayed immediately for determination of soluble acid invertase activity. For extraction of cell wall–bound acid invertase activity, the pellets were incubated for 20 hr with 5 volumes of extraction buffer containing 1 M NaCl in an orbital shaker at 4°C. The samples were then treated as described for the extraction of the soluble enzyme activity. Acid invertase activity was assayed by incubating aliquots of desalted extracts in a mixture containing acetate buffer (25 mM), pH 5.2, and 25 mM sucrose. Aliquots were removed after 20 and 40 min and boiled for 4 min to stop the reaction, and glucose quantification was performed as described above. Blanks were performed with heat-denatured extracts. Data were recorded only when linearity between glucose production and incubation time was observed.

Histochemical Analysis of Transgenic Plants

Transgenic potato plants harboring a gene coding β-glucoronidase (GUS) linked to the *invGE* promoter were obtained as described previously (Maddison et al. 1999). Stolons and developing tubers (1 to 3 cm diameter) from pot-grown plants were excised and histochemically assayed for GUS activity using the method of Jefferson et al. (1987) with the modifications described by Maddison et al. (1999).

REFERENCES

Appeldoorn, N.J.G., de Bruijn, S.M., Koot-Gronsveld, E.A.M., Visser, R.G.F., Vreugdenhil, D., and van der Plas, L. (1997). Developmental changes involved in conversion of sucrose to hexose-phosphate during early tuberization of potato. Planta **202,** 220–226.

Artschwager, E.F. (1924). Studies on the potato tuber. J. Agric. Res. **24,** 809–835.

Catchpole, A.H., and Hillman, J. (1969). Effect of ethylene on tuber initiation in *Solanum tuberosum* L. Nature **223,** 1387.

Cutter, E.G. (1978). Structure and development of the potato plant. In The Growth of the Potato, J.D. Ivins and F.L. Milthorpe, eds (London: Butterworth), pp. 99–113.

Davies, H.V. (1984). Sugar metabolism in stolon tips during early tuberization. Z. Pflanzenphysiol. **113,** 377–381.

Davies, H.V., and Oparka, K.J. (1985). Hexose metabolism in developing tubers of potato (*Solanum tuberosum* L.) cv Maris Piper. J. Plant Physiol. **119,** 311–316.

Davies, H.V., and Viola, R. (1994). Control of sugar balance in potato tubers. In The Molecular Biology of the Potato, 2nd edition, W.R. Belknap, M.E. Vayda, and W.D. Park, eds (Wallingford, UK: CAB International), pp 67–80.

Dwelle, R.B., Kleinkopf, G.E., and Pavek, J.J. (1981). Stomatal conductance and gross photosynthesis of potato (*Solanum*

tuberosum L.) as influenced by irradiance, temperature and growth stage. Pot. Res. **24,** 49–59.

Ehness, R., and Roitsch, T. (1997). Co-ordinated induction of mRNAs for extracellular invertase and a glucose transporter in *Chenopodium rubrum* by cytokinins. Plant J. **11,** 539–548.

Ewing, E.E. (1990). Induction of tuberization in potato. In The Molecular and Cellular Biology of the Potato, W.R. Belknap, M.E. Vayda, and W.D. Park, eds (Wallingford, UK: CAB International), pp. 25–41.

Ewing, E.E., and Struik, P.C. (1992). Tuber formation in potato: Induction, initiation and growth. Hortic. Rev. **14,** 89–198.

Fisher, D.B., and Cash-Clark, C.E. (2000). Sieve tube unloading and postphloem transport of fluorescent tracers and proteins injected into sieve tubes via severed aphid stylets. Plant Physiol. **123,** 125–137.

Fisher, D.B., and Oparka, K.J. (1996). Phloem unloading: Principles and problems. J. Exp. Bot. **47,** 1141–1154.

Frommer, W.B., and Sonnewald, U. (1995). Molecular analysis of carbon partitioning in solanaceous species. J. Exp. Bot. **46,** 587–607.

Gardner, A., Davies, H.V., and Burch, L.R. (1992). Purification and properties of fructokinase from developing tubers of potato (*Solanum tuberosum* L.). Plant Physiol. **100,** 178–183.

Hajirezaei, M.R., Takahata, Y., Trethewey, R.N., Willmitzer, L., and Sonnewald, U. (2000). Impact of elevated cytosolic and apoplastic invertase activity on carbon metabolism during tuber development. J. Exp. Bot. **51,** 439–445.

Hedley, P.E., Machray, G.C., Davies, H.V., Burch, L., and Waugh, R. (1993). cDNA cloning and expression of a potato (*Solanum tuberosum*) invertase. Plant Mol. Biol. **22,** 917–922.

Hedley, P.E., Machray, G.C., Davies, H.V., Burch, L., and Waugh, R. (1994). Potato (*Solanum tuberosum*) invertase-encoding cDNAs and their differential expression. Gene **145,** 211–214.

Herbers, K., and Sonnewald, U. (1998). Molecular determinants of sink strength. Curr. Opin. Plant Biol. **1,** 207–216.

Imlau, A., Truernit, E., and Sauer, N. (1999). Cell-to-cell and long-distance trafficking of the green fluorescent protein in the phloem and symplastic unloading of the protein into sink tissues. Plant Cell **11,** 309–322.

Jackson, S.D. (1999). Multiple signalling pathways control tuber induction in potato. Plant Physiol. **119,** 1–8.

Jefferson, R.A., Kavanagh, T.A., and Bevan, M.W. (1987). GUS fusions: β-Glucuronidase as a sensitive and versatile gene fusion marker in higher plants. EMBO J. **6,** 3901–3907.

Leshem, B., and Clowes, F.A.L. (1972). Rates of mitosis in shoot apices of potatoes at the beginning and end of dormancy. Ann. Bot. **36,** 687–691.

Maddison, A.L., Hedley, P.E., Meyer, R.C., Aziz, N., Davidson, D., and Machray, G.C. (1999). Expression of tandem invertase genes associated with sexual and vegetative growth cycles in potato. Plant Mol. Biol. **41,** 741–751.

Mingo-Castel, A.M., Smith, O.E., and Kumamoto, J. (1976). Studies on the carbon dioxide promotion and ethylene inhibition of tuberization in potato explants cultured *in vitro*. Plant Physiol. **57,** 480–485.

Mitchell, S., Dobson, P., Davies, H.V., and Viola, R. (1998). Potential for artefacts in the measurement of fructose and sucrose in extracts of potato tubers using the microplate reader assay. Pot. Res. **41,** 383–386.

Müller-Röber, B., Kossmann, J., Hannah, C.L., Willmitzer, L., and Sonnewald, U. (1990). One of two different ADP-glucose pyrophosphorylase genes from potato responds strongly to elevated sucrose levels. Mol. Gen. Genet. **224,** 134–146.

Müller-Röber, B., Sonnewald, U., and Willmitzer, L. (1992). Inhibition of the ADP-glucose pyrophosphorylase in transgenic potatoes leads to sugar-storing tubers and influences tuber formation and expression of tuber storage protein genes. EMBO J. **11,** 1229–1238.

Oparka, K. J. (1985). Changes in partitioning of current assimilate during tuber bulking in potato (*Solanum tuberosum* L.) cv Maris Piper. Ann. Bot. **55,** 705–713.

Oparka, K.J. (1986). Phloem unloading in the potato tuber. Pathways and sites of ATPase. Protoplasma **131,** 201–210.

Oparka, K.J., and Prior, D.A.M. (1987). ¹⁴C sucrose efflux from the perimedulla of growing potato tubers. Plant Cell Environ. **10,** 667–675.

Oparka, K.J., and Wright, K.M. (1988). Osmotic regulation of starch synthesis in potato tubers? Planta **174,** 123–126.

Oparka, K.J., Viola, R., Wright, K.M., and Prior, D.A.M (1992). Sugar transport and metabolism in the potato tuber. In Carbon Partitioning within and between Organisms, J.F. Farrar, A.J. Gordon, and C.J. Pollock, eds (Oxford, UK: BIOS Scientific Publishers), pp. 91–114.

Oparka, K.J., Roberts, A.G., Boevink, P., Santa Cruz, S., Roberts, I.M., Pradel, P., Imlau, A., Sauer, N., Kotlizky, G., and Epel, B. (1999). Simple, but not branched, plasmodesmata allow the nonspecific trafficking of proteins in developing tobacco leaves. Cell **97,** 743–754.

Park, W.D. (1990). Molecular approaches to tuberization in potato. In The Molecular and Cellular Biology of the Potato, W.R. Belknap, M.E. Vayda and W.D. Park, eds (Wallingford, UK: CAB International), pp. 43–56.

Patrick, J.W. (1997). Phloem unloading: Sieve element unloading and postphloem transport. Annu. Rev. Plant Physiol. Plant Mol. Biol. **48,** 191–222.

Prat, S., Frommer, W.B., Höfgen, R., Keil, M., Kossmann, J., Köster-Töpfer, M., Liu, X.J., Müller, B., Peña-Cortés, M., Rocha-Rosa, M., Sánchez-Serrano, J.J., Sonnewald, U., and Willmitzer, L. (1990). Gene expression during tuber development in potato plants. FEBS Lett. **286,** 334–338.

Roberts, A.G., Santa Cruz, S., Roberts, I.M., Prior, D.A.M., Turgeon, R., and Oparka, K.J. (1997). Phloem unloading in sink leaves of *Nicotiana benthamiana*. Comparison of a fluorescent solute with a fluorescent virus. Plant Cell **9,** 1381–1396.

Ross, H.A., and Davies, H.V. (1992). Sucrose metabolism in tubers of potato (*Solanum tuberosum* L.). Effects of sink removal and sucrose flux on sucrose-degrading enzymes. Plant Physiol. **98,** 287–293.

Ross, H.A., Davies, H.V., Burch, L.R., Viola, R., and McRae, D. (1994). Developmental changes in carbohydrate content and sucrose degrading enzymes in tuberizing stolons of potato (*Solanum tuberosum*). Physiol. Plant. **90,** 748–756.

Salanoubat, M., and Belliard, G. (1989). The steady-state level of potato sucrose synthase mRNA is dependent on wounding, anaerobiosis and sucrose concentration. Gene **84,** 181–185.

Sonnewald, U., Hajirezaei, M.R., Kossmann, J., Heyer, A., Tretehwey, R.N., and Willmitzer, L. (1997). Increased potato tuber size resulting from apoplastic expression of a yeast invertase. Nature Biotech. **15,** 794–797.

Sturm, A. (1999). Invertases. Primary structures, functions, and roles in plant development and sucrose partitioning. Plant Physiol. **121,** 1–7.

Tauberger, E., Hoffman-Benning, S., Fleischer-Notter, H., Willmitzer, L., and Fisahn, J. (1999). Impact of invertase overexpression on cell size, starch granule formation and cell wall properties during tuber development in potatoes with modified carbon allocation patterns. J. Exp. Bot. **50,** 477–486.

Viola, R. (1996). Hexose metabolism in discs excised from developing potato (*Solanum tuberosum* L.) tubers. I. Conversion of radiolabelled precursors can occur prior to uptake. Planta **198,** 179–185.

Viola, R., and Davies, H.V. (1992). A microplate assay for rapid enzymatic quantification of sugars in potato tubers. Pot. Res. **35,** 55–58.

Visser, R.G.F., Vreugdenhil, D., Hendriks, T., and Jacobsen, E.J. (1994). Gene expression and carbohydrate content during stolon to tuber transition in potatoes (*Solanum tuberosum*). Physiol. Plant. **90,** 285–292.

Vreugdenhil, D., and Struik, P.C. (1989). An integrated view of the hormonal regulation of tuber formation in potato (*Solanum tuberosum*). Physiol. Plant. **75,** 525–531.

Vreugdenhil, D., Xu, X., Jung, J.S., van Lammern, A.A.M., and Ewing, E.E. (1999). Initial anatomical changes associated with tuber formation on single-node potato (*Solanum tuberosum* L.) cuttings: A re-evaluation. Ann. Bot. **84,** 675–680.

Weber, H., Borisjuk, L., and Wobus, U. (1996). Controlling seed development and seed size in *Vicia faba*: A role for seed coat–associated invertases and carbohydrate state. Plant J. **10,** 823–834.

Wiltshire, J.J.J., and Cobb, A.H. (1996). A review of the physiology of potato tuber dormancy. Ann. Appl. Biol. **129,** 553–569.

Xu, J., Avigne, W.T., McCarty, D.R., and Koch, K. (1996). A similar dichotomy of sugar modulation and developmental expression affects both pathways of sucrose metabolism: Evidence from a maize invertase gene family. Plant Cell **8,** 1209–1220.

Xu, X., Vreugdenhil, D., and van Lammeren, A.M. (1998). Cell division and cell enlargement during potato tuber formation. J. Exp. Bot. **49,** 573–582.